# SUPPORTING INFORMATION

## Surpassing fundamental limits of oscillators using nonlinear resonators

L.G. Villanueva[1], E. Kenig[1], R.B. Karabalin[1], M.H. Matheny[1], Ron Lifshitz[2], M.C. Cross[1], M.L. Roukes[1]

[1]*Kavli Nanoscience Institute, California Institute of Technology, Pasadena, California 91125,*
[2]*Raymond and Beverly Sackler School of Physics, Tel Aviv University, 69978 Tel Aviv, Israel*

## SI-A. Amplitude equation

### 1. Externally driven resonator

The equation of motion of an externally driven nonlinear resonator is given by:

$$m\frac{d^2x}{dt^2}+\Gamma\frac{dx}{dt}+m\omega_0^2x+\tilde{\alpha}x^3=G\cos(\omega t) \tag{SI1}$$

where $x$ is the signal amplitude of the resonator, $m$ is its effective mass, $k=m\omega_0^2$ is its effective spring constant and resonance frequency respectively, $\tilde{\alpha}$ is the cubic spring constant, or Duffing parameter, $\Gamma$ is the linear damping rate and $\tilde{G}$ is the external driving force.

We are interested in solutions $\tilde{x}(t)$ that are slow modulations of the linear resonance oscillations and so we introduce a dimensionless slow time scale $T=\varepsilon\omega_0 t$ and displacement amplitude $A$: $\tilde{x}=\frac{1}{2}\tilde{x}_0A(T)e^{i\omega_0 t}+c.c.+\cdots$; where the small expansion parameter $\varepsilon$ and the displacement scale $\tilde{x}_0$ are chosen for convenience as detailed below, $c.c.$ stands for complex conjugate, and the ellipses $(\cdots)$ denote small corrections from higher harmonic that we will not need. Following the procedure outlined elsewhere[1], secular perturbation theory leads to the equation of motion for the slow modulations

$$\frac{dA}{dT}=-\frac{\gamma}{2}A+i\frac{3}{8}\alpha|A|^2A-i\frac{g}{2}e^{i\Omega T} \tag{SI2}$$

with

$$\gamma=\frac{\Gamma}{m\omega_0\varepsilon};\quad \alpha=\frac{\tilde{\alpha}x_0^2}{m\omega_0^2\varepsilon};\quad \Omega=\frac{\omega-\omega_0}{\varepsilon\,\omega_0};\quad g=\frac{G\tilde{\alpha}}{\varepsilon^{3/2}\omega_0^3m^{3/2}}. \tag{SI3}$$

For the expansion procedure to be consistent $\gamma,\alpha$ must be $O(1)$ quantities. Thus we choose the scale factors $\varepsilon=\Gamma/m\omega_0=Q^{-1}$ and $x_0^2=m\omega_0^2/\tilde{\alpha}Q$ so that in the absence of fluctuations the values of $\gamma,\alpha$ are unity. In the presence of parameter fluctuations in $\Gamma$ and $\tilde{\alpha}$ this leads to: $\gamma=1+\Xi_\gamma(T)$ and $\alpha=1+\Xi_\alpha(T)$, with $\Xi_\gamma,\Xi_\alpha$ representing the slow time noise

sources characterizing the fluctuations. As the amplitude is locked to the driving force, we can also express it as $A = ae^{i\varphi}e^{i\Omega T}$ and therefore obtain:

$$\frac{da}{dT} + i\Omega a = -\frac{\gamma}{2}a + i\frac{3}{8}\alpha a^3 - i\frac{g}{2}e^{-i\varphi} \tag{SI4}$$

## 2. Heavily saturated oscillator

We reproduce all the previous steps to arrive at the amplitude equation describing the slow-time motion of a heavily saturated oscillator, which is:

$$\frac{dA}{dT} = -\frac{\gamma}{2}A + i\frac{3}{8}\alpha|A|^2A - i\frac{s}{2}\frac{A}{|A|}e^{i\Delta}, \tag{SI5}$$

with $s$ being the saturation level of the feedback function and $\Delta$ the phase delay present in the feedback loop. We substitute $A = ae^{i\phi(T)}$ into Eq. (SI5), which yields:

$$\frac{da}{dT} + i\frac{d\phi}{dT}a = -\frac{\gamma}{2}a + i\frac{3}{8}\alpha a^3 - i\frac{s}{2}e^{i\Delta}. \tag{SI6}$$

It is clear that Eqs. (SI4) and (SI6) are equivalent, however, in the case of an externally driven resonator, the control parameters determining the motion are the driving frequency $\Omega$ and amplitude $G$; while in the case of a heavily saturated oscillator, those parameters are the feedback phase $\Delta$ and amplitude $s$, see Figure S1.

It is also possible to separate Eq. (SI6) into real and imaginary parts to obtain:

$$\begin{aligned} \frac{da}{dT} &= -\frac{\gamma a}{2} + \frac{s}{2}\sin\Delta = f_a; \\ \Omega = \frac{d\phi}{dT} &= \frac{3\alpha}{8}a^2 - \frac{s}{2}\frac{\cos\Delta}{a} = f_\phi; \end{aligned} \tag{SI7}$$

where $\Omega$ is the oscillation frequency. After the steady state is reached, we obtain:

$$\begin{aligned} a &= \frac{s}{\gamma}\sin\Delta\,; \\ \Omega &= \frac{3\alpha}{8}a^2 - \frac{s}{2}\frac{\cos\Delta}{a}; \end{aligned} \tag{SI8}$$

which is Eq. (1) in the main manuscript, describing the limit cycle of a heavily saturated oscillator.

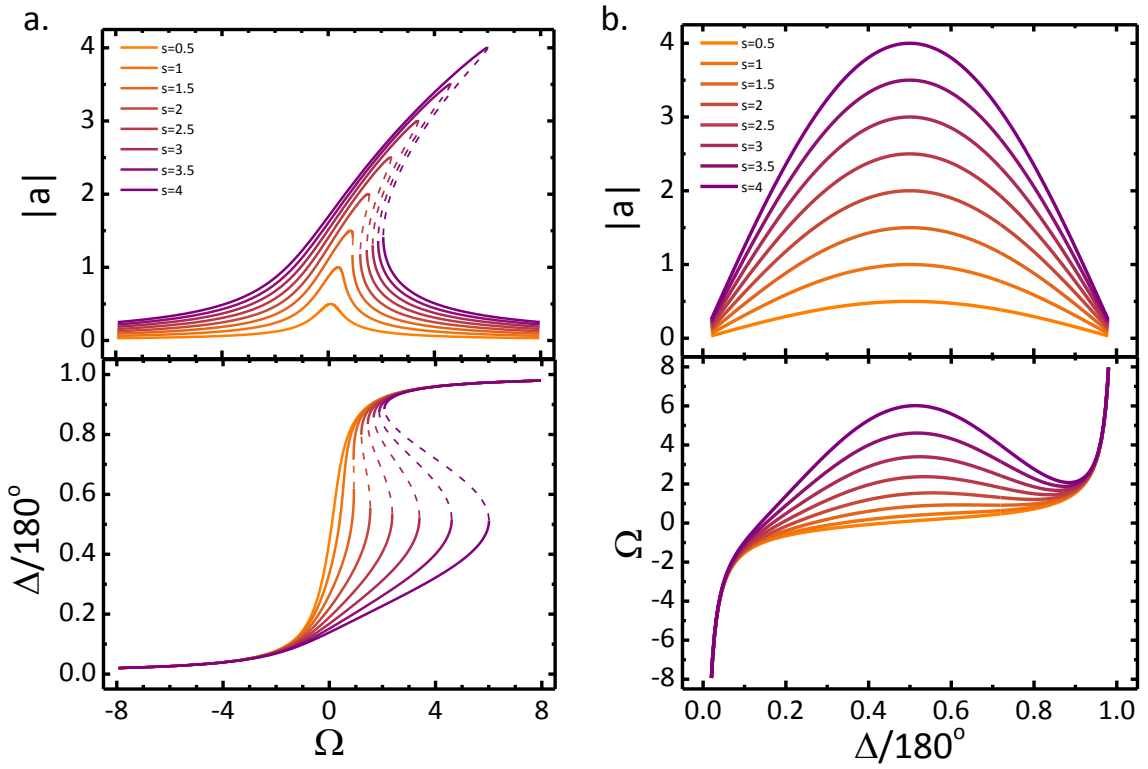


**Figure S1** Resonant response curves showing the differences between an externally driven resonator (a) where the dynamics are determined by the frequency (Ω) of the external force; and a heavily saturated oscillator (b), where the operational point is determined by the feedback phase. It is therefore possible to see that in the first case (a) there are regions with several solutions and one of them is unstable (dashed lines), whereas in the second case both amplitude and frequency are single-valued functions of the phase, so no instability is found.

## SI-B. Location of optimized operational points

Using the expressions in Table 1 of the main manuscript, we can easily find the sets of operational points that minimize the contribution to phase noise coming from noise in parameter Δ and coming from thermomechanical noise through amplitude-phase conversion. We present those sets in the following Figure S2.

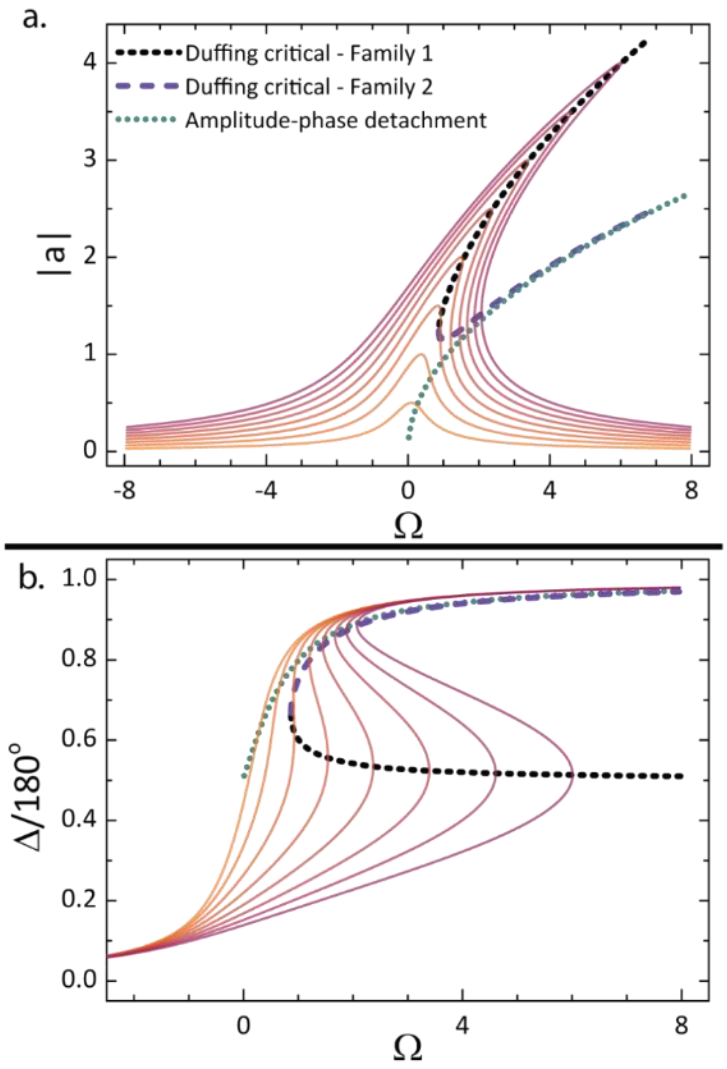


**Figure S2** Operational points of a heavily saturated oscillator, highlighting the sets of points where different contributions to the phase noise are canceled, in particular the contribution due to fluctuations in Δ and the contribution due to amplitude-phase converted thermomechanical noise. Notice how the second family of DCPs approaches the ADP set for high levels of drive.

# SI-C. Experimental determination of noise intensities

## 1. Thermomechanical noise

Thermomechanical noise enters the dynamical equations as a random force $\xi_{Th}(t)$, so Eq. (SI1) can be written including this noise term as:

$$m\frac{d^2x}{dt^2} + \Gamma\frac{dx}{dt} + m\omega_0^2 x + \tilde{\alpha}x^3 = G\cos(\omega t) + \xi_{Th}(t) \tag{SI9}$$

where the magnitude of the noise is imposed by the fluctuation-dissipation theorem: $\langle\tilde{\xi}_{Th}(\tilde{t})\tilde{\xi}_{Th}(\tilde{t}')\rangle = 2\Gamma k_B\mathcal{T}\delta(t-t')$, where $k_B$ is the Boltzmann constant and $\mathcal{T}$ is the temperature. If we apply the rescaling steps described before and elsewhere[1], we end up with the following amplitude equation with noise:

$$\frac{dA}{dT} = f(A) + \Xi_{Th}(T) \tag{SI10}$$

where $f(A)$ are the deterministic terms described previously and $\Xi_{Th}(T)$ is the dimensionless equivalent of $\tilde{\xi}_{Th}(\tilde{t})$. $\Xi_{Th}(T)$ is a complex quantity ($\Xi_{Th} = \Xi_R + i\Xi_I$) that defines the intensity of the noise for our model as:

$$\langle\Xi_R(T)\,\Xi_R(T')\rangle = \langle\Xi_I(T)\,\Xi_I(T')\rangle = I_{Th}\delta(T-T') \tag{SI11}$$

with $I_{Th} = \frac{k_B\mathcal{T}Q_0\tilde{\alpha}_0}{m^2\omega_0^4}$. In order to estimate $I_{Th}$ we measure the frequency $\omega_0$ and quality factor $Q_0$ through a linear resonant sweep. We estimate the mass, $m$, through careful inspection in a scanning electron microscope (SEM) to determine the beam's dimensions, as well as through subsequent finite element modeling (FEM) simulations. Finally, we estimate $\tilde{\alpha}_0$ following the method detailed elsewhere[2], by analyzing the resonant responses for increasing drive levels.

Assuming that the beam remains at room temperature (as suggested by FEM results for the temperature distribution for the voltages used in these experiments), the intensity of thermomechanical noise is:

$$I_{Th} \approx 1.5\cdot 10^{-5} \tag{SI12}$$

## 2. Noise in Δ

To estimate the magnitude of the noise in the feedback phase $I_\Delta$, we first characterize the phase noise introduced by different components in the feedback loop. We do that by comparing the phase noise of a monotonic signal from an Agilent N5180 to that same signal after passing the component under test. We find that the contribution from other components are negligible compared to that of the resonator transduction and the first low noise amplifier in the gain chain.

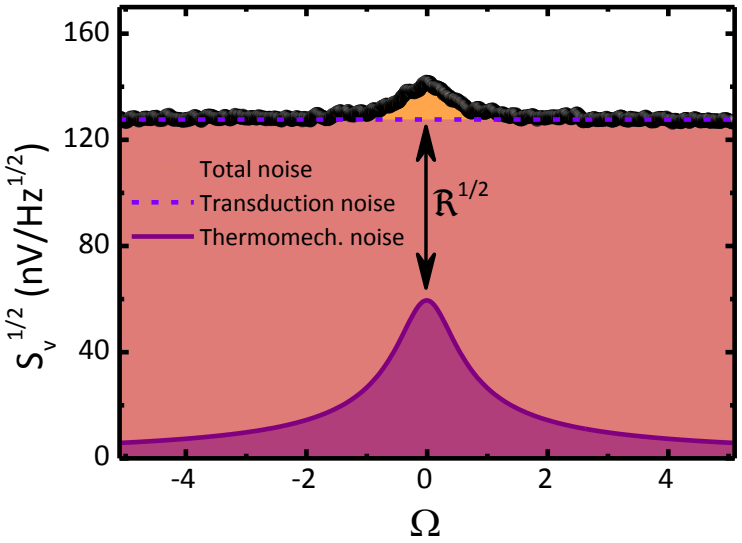


**Figure S3** Thermomechanical and system (or transduction) noise in our resonator after first amplifier stage in the gain chain.

In a linear gain chain, the noise in Δ is evaluated as the ratio between the non-thermal noise in the signal and the squared oscillation amplitude: $I_\Delta = S_a/a^2$. By measuring the noise after the first amplifier stage, we can calibrate the transduction noise using the thermomechanical noise (see Figure S3), giving $I_\Delta = 4I_{Th}\Re/a^2$, with $\Re \approx 4.5$. However, as we have described, our gain chain is not linear but operates in the heavily saturated regime. By considering a $\tanh(x)$ amplifier gain curve in the highly saturated limit, we obtain:

$$I_\Delta \approx \frac{8}{3}\frac{I_{Th}\Re}{a \cdot s} \approx 12\frac{I_{th}}{a \cdot s} \qquad \text{(SI13)}$$

but the actual proportionality coefficient in Eq. (SI13) might be slightly different depending on the actual amplifier gain curve.

## 3. Noise in $s$

Noise in the magnitude of the output signal of the linear amplifier stages is suppressed by the subsequent limiter and variable attenuator. However these elements may also add noise, resulting in noise in the saturation parameter $s$. We estimate this noise in the saturation parameter $s$ by sending a monotonic signal from an Agilent N5180 through the limiter and variable attenuator. We compare the phase noise and the power spectrum of the signal before and after the limiting stage. While phase noise affects both measurements, noise in $s$ is only visible in the power spectrum. We observe, however, the same result in both measurements, approximately $2.5 \cdot 10^{-12}\ V^2/\text{Hz}$ when the saturation level is 28.15 mV, corresponding to $s = 3.473$. This implies that the noise in the saturation level should be smaller than $\zeta = 10^{-13}\ V^2/\text{Hz}$. Translating to the scaled variables we can now write:

$$I_s = \frac{\omega_0}{Q}\left(\frac{s}{28.15\ \text{mV}}\right)^2 \zeta \leq 6 \cdot 10^{-5} \qquad \text{(SI14)}$$

## 4. Adjustment of the noise intensities

Using the expressions Table 1 in the main manuscript, and the intensities calculated above; we can predict the total phase noise by adjusting the rest of the intensities.

We first consider only the contributions from thermomechanical noise and noise in $\Delta$ for which we have independent estimates. We find that either one of these two noise sources dominates the phase noise across the whole explored parameter space, except for a small region about the optimal operating point. To optimize the fitting we set $I_{Th} = 1.5 \cdot 10^{-5}$ and $I_\Delta = 9\frac{I_{th}}{a \cdot s}$. For the latter, the slight difference (9 versus 12) with the value estimated in Eq. (SI13) is motivated to improve the fitting for small values of saturation. We then focus on the region close to ADP and DCP-2 where these two noise sources are insufficient to account for the measured oscillator noise to obtain a value of the noise in the frequency parameter: $I_{\omega_0} = 0.7 \cdot 10^{-4}$.

Finally, we study the region around $\Delta = 90^o$, and we see that to obtain a better fit with the experimental data, noise in the saturation parameter needs to be much smaller than the upper bound set by Eq. (SI14). However the consequence is that we need some other source of noise that grows much faster with the saturation level than the noise in the saturation. Looking at Table 1, we see that both noise in $\alpha$ and $\gamma$ grow faster than noise in $s$, and so we set both fluctuations to be around $\sim 10^{-6}$. Choosing fluctuations in $\gamma$ to be slightly larger provides a much better match to the experiments. The final values for the intensities were: $I_s \sim 5 \cdot 10^{-6},\ I_\alpha = 10^{-6}, I_\gamma = 2 \cdot 10^{-6}$.

## SI-D. Effect of fluctuations in frequency

As discussed in the main manuscript, we observe an improvement in the phase noise at larger driving power (beyond the nonlinear threshold). This improvement, however, is bounded by fluctuations in the resonance frequency of the device itself. If these device fluctuations were to be cancelled or reduced, the improvement would be much more significant. In the following figure we present the comparison of the predictions of the model with and without the contribution due to fluctuations in the resonance frequency.

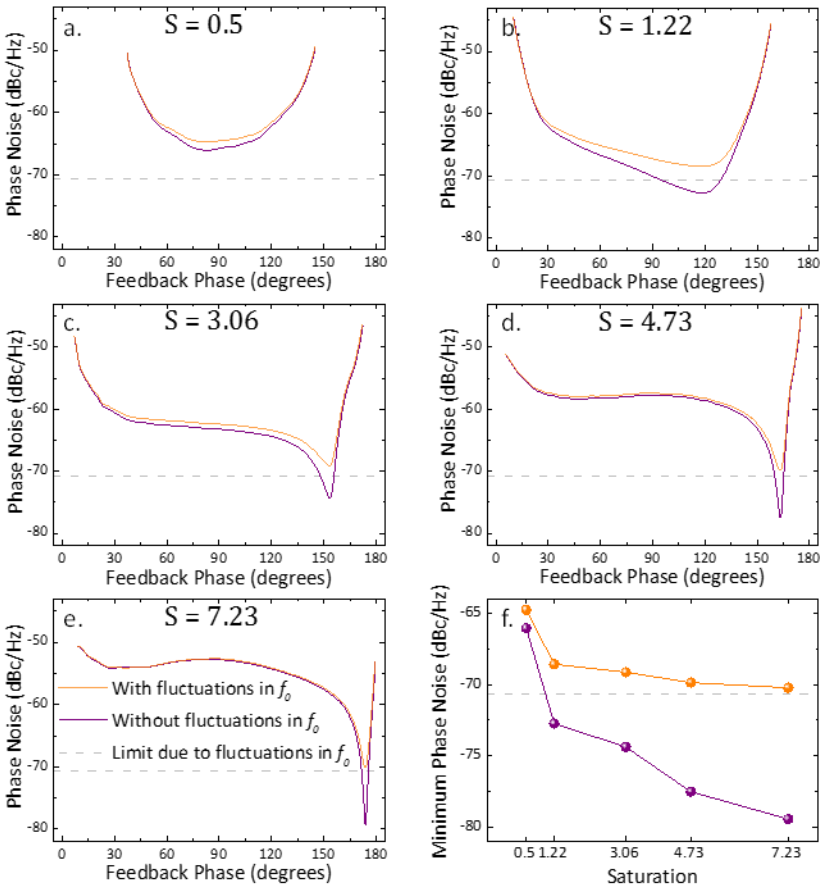


**Figure S4** (a-e) Comparison of the model prediction for the total phase noise accounting for (orange) and not accounting for (purple) frequency fluctuations of the mechanical device. (f) Shows the minimum phase noise for each saturation value. It can be clearly seen how the frequency fluctuations soon become the limiting factor. An improvement of 10 dBc/Hz should be possible if the fluctuations in frequency were minimized.

## SI-E. References

1. Lifshitz, R. & Cross, M.C., *Nonlinear Dynamics of Nanomechanical and Micromechanical Resonators*, in *Reviews of nonlinear dynamics and complexity*, H.G. Schuster, Editor. 2008, Wiley-VCH: Weinheim.
2. Matheny, M.H., Villanueva, L.G., Karabalin, R.B., Sader, J.E. & Roukes, M.L. Generalized System for the Measurement of Nonlinearities in Nanomechanical Devices. *submitted* **99,** (2012).